JOURNAL OF MATERIALS SCIENCE 25 (1990) 1877–1885

Plastic behaviour of $Cd_xHg_{1-x}Te$ ($0 \leqslant x \leqslant 1$) crystals

J. F. BARBOT, G. RIVAUD, H. GAREM, C. BLANCHARD, J. C. DESOYER
Laboratoire de Métallurgie Physique, U.A.131 CNRS, Faculté des Sciences, 86022 Poitiers Cedex, France

D. LE-SCOUL, J. L. DESSUS, A. DURAND
S. A. Télécommunications, Av. des Hauts de la Chaume, 86280 Saint-Benoît, France

$Cd_xHg_{1-x}Te$ ($0 \leqslant x \leqslant 1$) single crystals were strained by microhardness and by constant strain rate uniaxial compression tests, in the temperature range 300 to 600 K. Hardness curves as function of temperature can be described by empirical relations. Stress–strain curves, relaxation tests and dislocation observations using transmission electron microscopy show that the deformation is controlled by a thermally activated Peierls mechanism. Moreover, dislocations are dissociated with a stacking fault energy which does not depend on the x composition.

1. Introduction

Dislocations are crystalline defects, which can strongly modify density, mobility and lifetime of charge carriers. Semiconductor devices are expected to suffer from these defects so that efforts were devoted to eliminate them. Knowledge of dislocation structure, mobility, multiplication and the processes by which they move in the material is necessary to allow for the elimination of these defects. Studying plastic deformation contributes to get a better understanding of the dislocation behaviour.

Several microscopic mechanisms can control the mobility of glide dislocations in crystals. It is now well established that the mechanism involved in plastic deformation, at "low" temperature, of semiconducting III–V compounds is the Peierls mechanism, whereas the I–VII compounds deformation is known to be controlled by the interaction of dislocations with point defects or impurities. In this context, II–VI compounds which have an ionicity close to that of alkali halides are interesting to investigate. Some works have been devoted to the plastic deformation on II–VI binary compounds, especially on CdTe [1, 2], ZnTe [3], ZnSe [4] and ZnS [5, 6] which show that a Peierls type mechanism may be involved in the deformation process. Moreover, dislocation studies using electron microscopy in plastically deformed II–VI compounds have shown that dislocations are dissociated with a stacking fault energy γ, which is about 10 to 15 mJ m^{-2}.

The $Cd_xHg_{1-x}Te$ (CMT) II–VI compounds are interesting alloys for plastic deformation investigations thanks to their ionicity factor f_i which varies between 0.65 (for HgTe) and 0.717 (for CdTe) [7] as a function of composition x. Few informations on the mechanical properties of ternary semiconductor compounds and especially on CMT are available although they are materials of interest for photodetectors and optoelectronic devices. Indeed, CMT band gap varies continuously from about 1.5 eV (CdTe) down to less than 0.05 eV ($x \approx 0.1$) which corresponds to wavelengths from 0.9 to 25 μm. The main application is the infrared detection through the two atmospheric windows 8–12 μm for $x \approx 0.2$ and 3–5 μm for $x \approx 0.3$. The composition $x \approx 0.7$ (corresponding to the wavelength 1.35 μm) is well suited for fibre optic signal transmission.

In a previous work [8] we have investigated, using Microhardness testing at room temperature, the plastic behaviour of CMT single crystals. A hardness maximum for $x \approx 0.75$ has been confirmed and the hardness polarity observed on {1 1 1} CMT faces has been explained in terms of dislocation mobilities. Cole *et al.* [9] have also reported plastic flow in $Cd_xHg_{1-x}Te$ ($0.18 \leqslant x \leqslant 0.3$) by four point bending testing in the temperature range 293 to 468 K.

In the present paper we report a detailed study of the macroscopic and microscopic mechanical behaviour of CdHgTe ($0 \leqslant x \leqslant 1$) grown by the travelling heater method (THM). Two techniques have been used: microindentation and uniaxial compression at constant plastic strain rate. These techniques have been applied to CMT single crystals from room temperature up to about 600 K. Stress relaxation tests have also been performed during compression testing in order to identify the microscopic mechanisms controlling the deformation. The strained samples have thus been examined by TEM in order to observe the dislocation configurations and the microstructures as a function of deformation conditions.

In addition, photoplastic effect (PPE) experiments on $Cd_{0.2}Hg_{0.8}Te$ have been performed during compression tests; results are shown in [10].

2. Experimental conditions

Composition of CMT alloys grown by THM was

0022–2461/90 $03.00 + .12

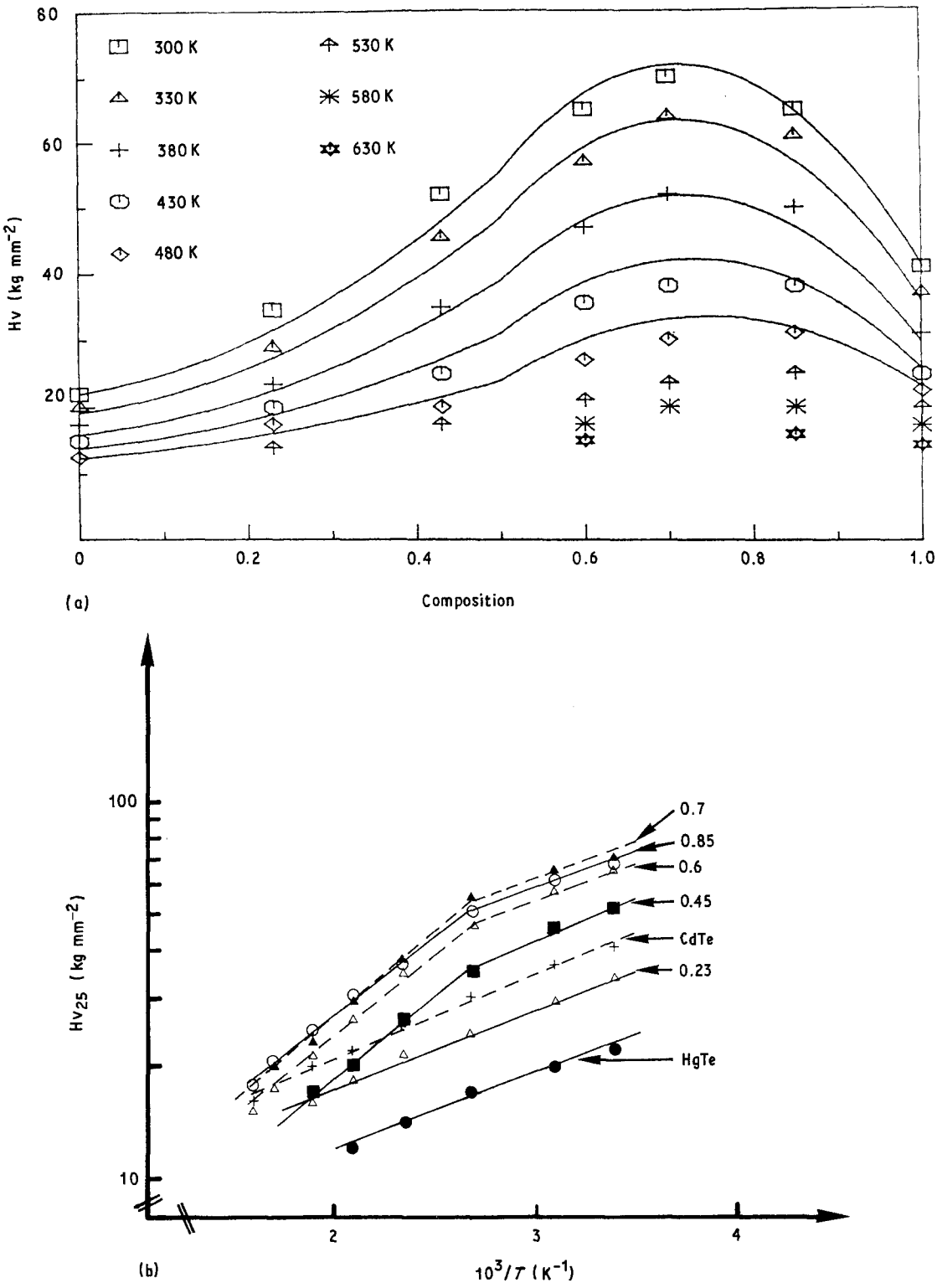

Figure 1 (a) Microhardness H_v of $Cd_xHg_{1-x}Te$ against composition as function of temperature ($300 \leqslant T \leqslant 630$ K). Experimental data are compared with curves obtained from Equations 1, 2, 3 and 4 (see text). (b) $\mathrm{Ln}(H_v(x))$ against inverse temperature for CMT.

controlled by infrared optical transmission and the homogeneity obtained by IR optical cartography. CdTe was grown from the melt using a modified Bridgman growth process. Electrical characterization was performed using Hall measurements at 77 and 300 K.

2.1. Microhardness tests

Slices, 1 mm thick, used for microhardness experiments were mechanically and chemically polished in 5 vol% bromine in methanol for one minute to remove surface damage. Microhardness tests were conducted under argon atmosphere using a Vickers indentor and load of 25 g for 20 s.

2.2. Uniaxial compression

Physical characteristics of studied samples are listed in Table I. For the CMT ($x = 0.2$ and 0.66), the initial dislocation density was estimated to be about 10^5–10^6 cm^{-2} by etching on the $\{1\,1\,1\}$ A face. Samples were cut in the form of parallelepiped ($2.5 \times 2.5 \times 5.5$ mm^3), with $[\bar{1}\,2\,3]$ compression axis in order to

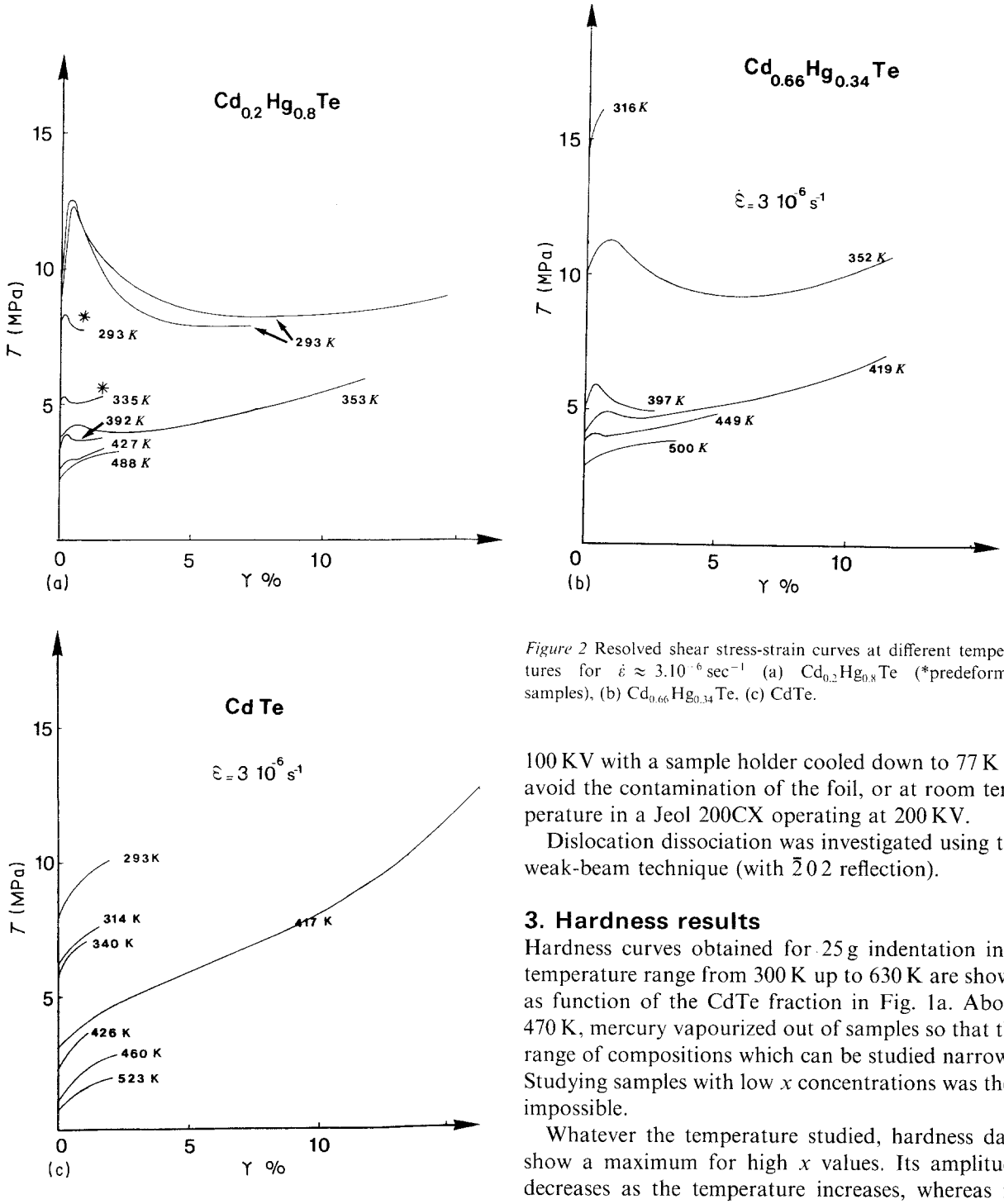

Figure 2 Resolved shear stress-strain curves at different temperatures for $\dot{\varepsilon} \approx 3.10^{-6}\,sec^{-1}$ (a) $Cd_{0.2}Hg_{0.8}Te$ (*predeformed samples), (b) $Cd_{0.66}Hg_{0.34}Te$, (c) CdTe.

favour simple slip of the dislocations of the $1/2[\bar{1}\,0\,1]$ $(1\,1\,1)$ glide system. They were also mechanically and chemically polished.

Compression tests were conducted in air using an Instron machine in a temperature range from 293 to 550 K. Stress relaxation tests were performed by stopping, during the compression, the cross-head and recording the load versus time curve.

2.3. Transmission electron microscopy

Deformed samples ($x = 0.2$ and 0.66) were cut in slices about 100 μm parallel to the primary slip plane. Electron transparent areas were prepared by ion milling (3.5 KV, $T = 77$ K) or by chemical procedure in a jet polisher operating at low jet speed (0.05 vol% bromine in methanol). Observations were made in a Philips EM300 electron microscope operating at 100 KV with a sample holder cooled down to 77 K to avoid the contamination of the foil, or at room temperature in a Jeol 200CX operating at 200 KV.

Dislocation dissociation was investigated using the weak-beam technique (with $\bar{2}\,0\,2$ reflection).

3. Hardness results

Hardness curves obtained for 25 g indentation in a temperature range from 300 K up to 630 K are shown as function of the CdTe fraction in Fig. 1a. Above 470 K, mercury vapourized out of samples so that the range of compositions which can be studied narrows. Studying samples with low x concentrations was then impossible.

Whatever the temperature studied, hardness data show a maximum for high x values. Its amplitude decreases as the temperature increases, whereas its position, about $x \approx 0.7$, does not seem to vary. This effect is also observed on $Zn_xHg_{1-x}Te$ ($0 \leqslant x \leqslant 1$) ternary alloys [11]. We note that this hardness peak disappears at 630 K.

An Arrhenius plot showing the ln (hardness) as a function of inverse temperature is plotted in Fig. 1b. For x compositions corresponding to the hardness maximum, a very marked feature of the data is the change in slope at about 460 K, whereas the data

TABLE I Physical characteristics of studied CMT single crystals

x	E_G(eV) (300 K)	T_M(K)	doping (cm^{-3})	a_0(A)
0.2	0.15	980	$p \approx 10^{15}$	6.464
0.66	0.8	1100	$p \approx 10^{15}$	6.474
1	1.5	1340	n	6.482

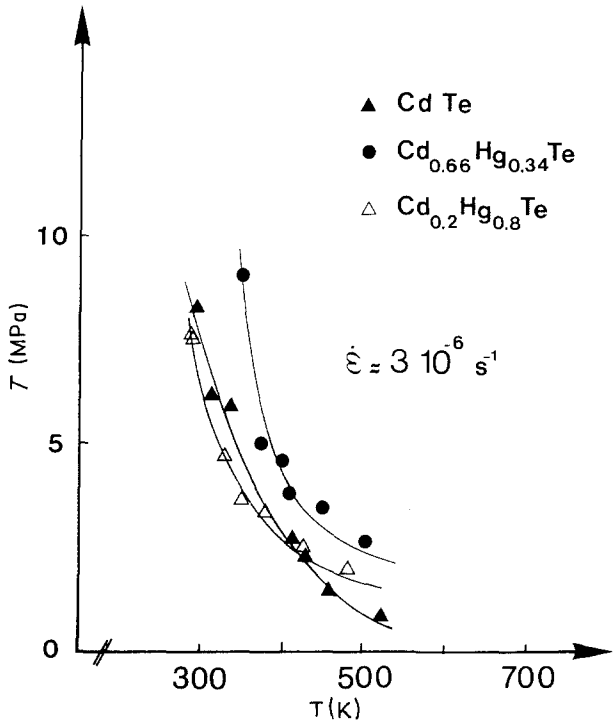

Figure 3 Dependence of τ^*_{Ly} on temperature T.

obtained for other compositions can be aligned over the temperature range studied. It is thus possible to determine an activation energy from an expression $H_v \propto \exp(E/kT)$, E being the activation energy governing plastic flow. For compositions showing a maximum in hardness, activation energies have been determined in the temperature range below 460 K to be about 0.09 eV. At upper temperatures and for other compositions, it has been found about 0.04 eV.

At $T = 300$ K, hardness variations against composition can be described by the following equations:

$$\text{for} \quad 0 \leqslant x \leqslant 0.5$$

$$H_v(x) = [H(1) - H(0)]x + H(0) + k_1 x^2 \quad (1)$$

$$\text{for} \quad 0.5 < x \leqslant 1$$

$$H_v(x) = [H(1) - H(0.5)]\,(2x - 1) + H(0.5) + k_2(1 - x)(x - 0.5) \quad (2)$$

Equation 1 has been proposed by Shenk *et al.* [12] while Equation (2) is deduced from the empirical relation for an ideal solid solution [13]. $H(0.5)$ is calculated from Equation (1), $H(1)$ and $H(0)$ being microhardness of pure components. Hardness variations as a function of temperature can be described by the experimental relation (3) previously determined:

$$H_v(T) = H_0 \exp(E/kT) \quad (3)$$

Moreover, if we choose a linear law for k_1 and k_2 as function of temperature, i.e.

$$k_{1,2}(T) = a_{1,2}T + b_{1,2} \quad (4)$$

we note, according to Fig. 1a, that our $H_v(x, T)$ experimental data agree quite well with hardness curves calculated using the four equations above mentioned. H_0, $a_{1,2}$ and $b_{1,2}$ are experimentally determined constants.

Cole *et al.* [13] propose that the solid solution

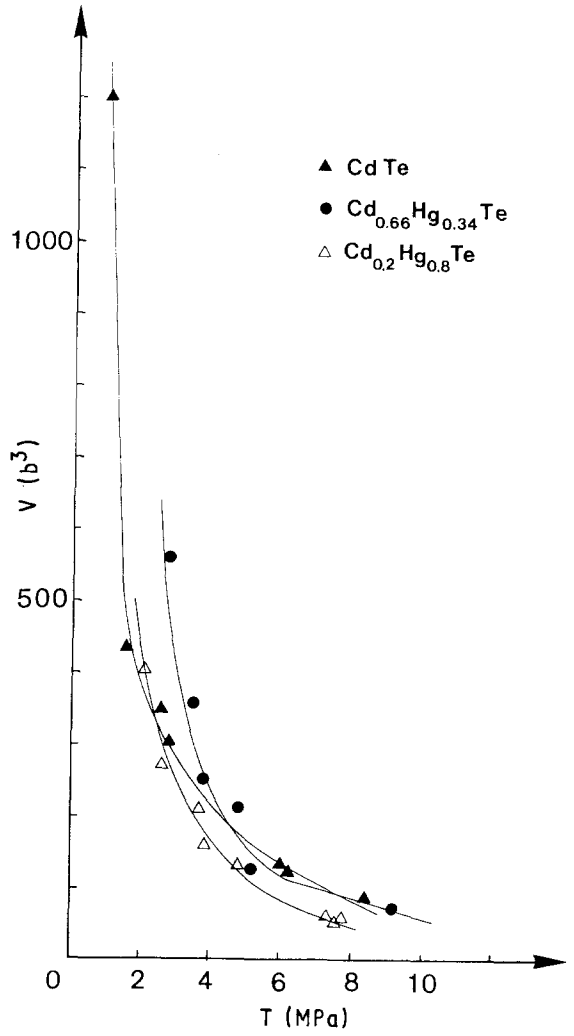

Figure 4 Variation of activation volume with the resolved shear stress τ^*_{Ly}.

hardening in CMT alloys may arise from elastic and electrical interactions of solute atoms with dislocations. Schenk *et al.* [12] additionally suggest a quasi-superstructure of the (3Cd : 1Hg)Te tetrahedron type and, moreover, a quasi-long-range order of these tetrahedrons about the composition $x \approx 0.7$. Ordering has previously been considered by Balagurova *et al.* [14]. In addition, Zax *et al.* [15] have recently demonstrated, using High-resolution solid–state NMR experiments, that Hg and Cd atoms do not distribute themselves randomly in the alloy lattice.

4. Uniaxial compression results ($\dot{\varepsilon} \approx 3.10^{-6}\,sec^{-1}$)

Samples were strained with a cross-head speed $v_t = 10^{-1}$ mm min^{-1}, corresponding to a strain rate $\dot{\varepsilon} \approx 3.10^{-6}\,sec^{-1}$.

4.1. Stress–strain curves

$\tau(\gamma)$ curves obtained from 293 K up to 500 K for compositions $x = 0.2$, 0.66 and 1 are shown in Figs 2a, b and c respectively, from which the following points can be derived:

(i) For compositions $x = 0.2$ and 0.66 the curves exhibit a marked yield point followed by a zero work hardening regime, similar to those observed commonly for other semiconductors with low initial dislocation

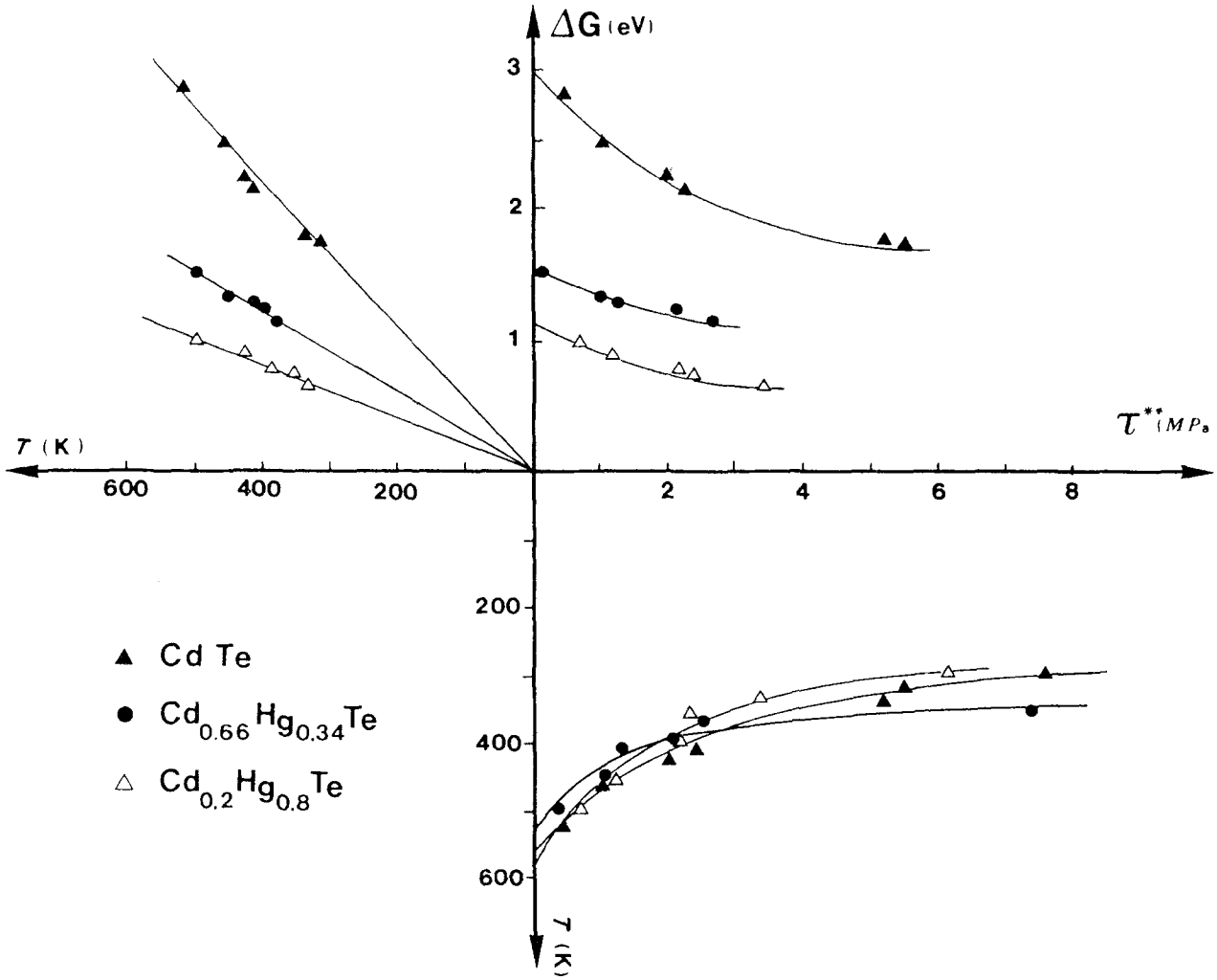

Figure 5 Cross diagram for $Cd_xHg_{1-x}Te$: $\Delta G(T)$, $\Delta G(\tau^{**})$ and $\tau^{**}(T)$.

density. A predeformation of about 1% reduces strongly its magnitude. No yield drop appears for CdTe, probably owing to the high initial density of dislocations.

(ii) $Cd_{0.66}Hg_{0.34}Te$ is brittle at low temperature. At 316 K ($T \approx 0.29\,T_M$) the samples fail for a stress of about 16 MPa. After a predeformation $\approx 2\%$ at 500 K, samples do not exhibit any plastic deformation at room temperature.

(iii) τ increases strongly as the temperature decreases which indicates a thermally activated deformation process.

4.2. Temperature dependence of the shear stress

The corrected shear stresses τ^*_{Ly} are plotted as a function of temperature in Fig. 3. Stress levels decrease rapidly with increasing temperature. Athermal regimes do not seem to be reached at the highest investigated temperatures, nevertheless they can be estimated to be about 600 K. Athermal stresses τ^*_μ are listed in Table II.

TABLE II Values of athermal stress τ^*_μ, barrier height ΔG_0 and α coefficient against cadmium concentration x

x	τ^*_μ(MPa)	α	ΔG_0(eV)
0.2	1.5	23	1.1
0.66	2	35	1.6
1	0.5	64	3

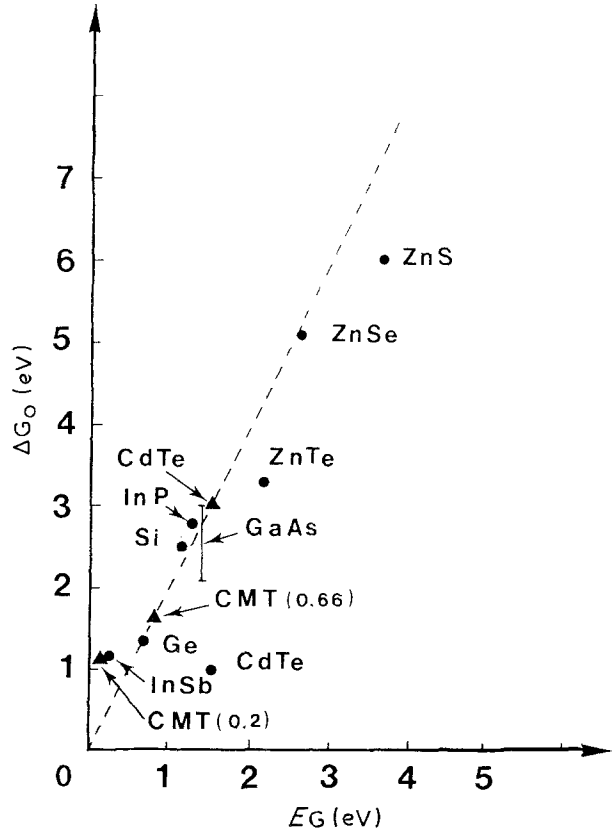

Figure 6 Relationship between activation energy and band gap (Gilman [17]); Si [18]; InSb [19]; InP [20]; GaAs [21, 22]; CdTe [24]; our results ▲ [23], ZnTe, ZnSe, ZnS.

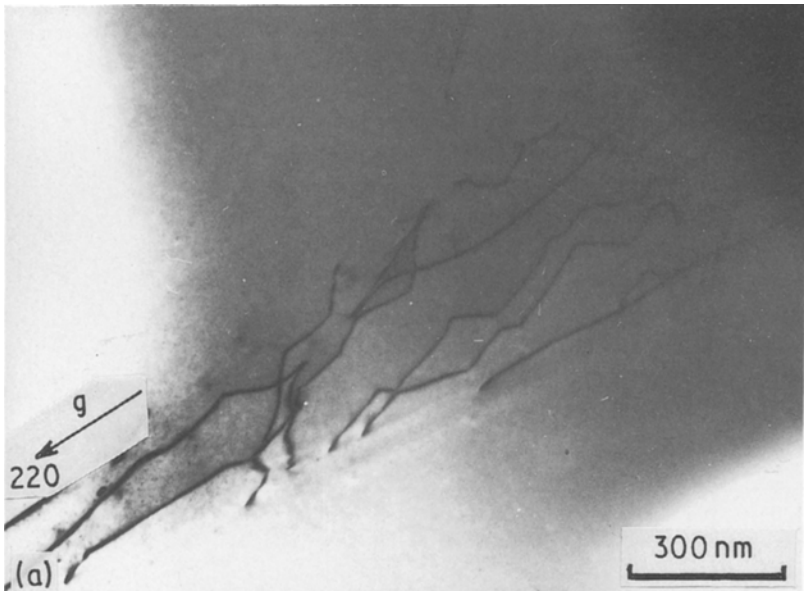

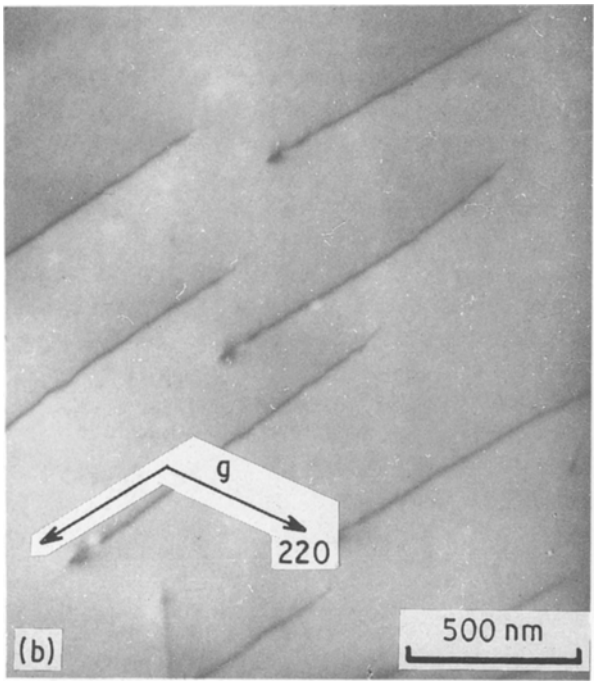

Figure 7 Dislocation microstructures observed in $Cd_{0.66}Hg_{0.34}Te$ deformed at 316 K. Observations at 100 KV. (a) Glide band, (b) individual dislocations.

Note also that the relative difference between composition $x = 0.2$ and 0.66 decreases as the temperature increases. These results confirm the data obtained with microhardness experiments.

4.3. Stress relaxation tests

Activation volumes have been evaluated experimentally using relaxation tests equation $V = kT(\delta \ln \dot{\gamma}/\delta\tau)_T$. Figure 4 shows the corresponding activation volume (estimated to within $\pm 15\%$) versus the flow stress τ^*_{Ly}. The curves are hyperbolic, activation volumes are small ($< 100\,b^3$) for high stresses (low temperatures) and increase rapidly when stress magnitude decreases.

4.4. Activation parameters analysis

A complete analysis can be developed assuming that plasticity can be described by the apparent state equation

$$\dot{\gamma} = \dot{\gamma}_0 \exp(-\Delta G(\tau, T)/kT)$$

where $\Delta G(\tau, T)$ is the apparent activation enthalpy. From variations of activation volumes and of shear stresses τ^*_{Ly} as a function of temperature, $\Delta G(T)$ can be deduced. $\Delta G(T)$ shows a linear variation depicted by an equation in the form $\Delta G(T) = \alpha kT\,\alpha$ values are listed in Table II. For dislocation densities between 10^3 to $10^8\,cm^{-2}$ Groh [16] has shown that $\alpha = \ln(\dot{\gamma}_c/\dot{\gamma})$ is about 25 to 35. Experimental α values found for $x = 0.2$ and 0.66 are in agreement with this evaluation whereas the one obtained for CdTe is very high.

Moreover, the extrapolation of $\Delta G(\tau^{**})$ curves toward zero, where τ^{**} is the thermal stress, gives height barriers ΔG_0 that impede the dislocation motion. All results are plotted in a cross-diagram, Fig. 5. Values of ΔG_0 are shown in Table II. For covalent crystals, Gilman [17] has shown that the activation energy for plastic flow equals twice the energy gap. For $x = 0.66$ and 1 the values of ΔG_0 agree well with this empirical correlation. This does not hold for the compound $Cd_{0.2}Hg_{0.8}Te$, this last one however is closer to a semimetal than a semiconductor. In Fig. 6 we have also plotted some activation enthalpy values of covalents, III–V and II–VI compounds reported in the literature [17–23]. Note also that for different deformation conditions Maeda *et al.* [24] have found an activation enthalpy of CdTe of about 1 eV. However, this parameter is particularly sensitive to the material purity.

5. TEM observations

Observations of dislocations in plastically deformed CMT compounds have been performed using transmission electron microscopy.

(i) $x = 0.66$

At 316 K ($\tau \approx 16$ MPa, $\gamma \approx 0.3\%$) the dislocation density is low and extremely inhomogeneous showing that the deformation is heterogeneous. Dislocations are localized in the glide plane, Fig. 7a, in the low

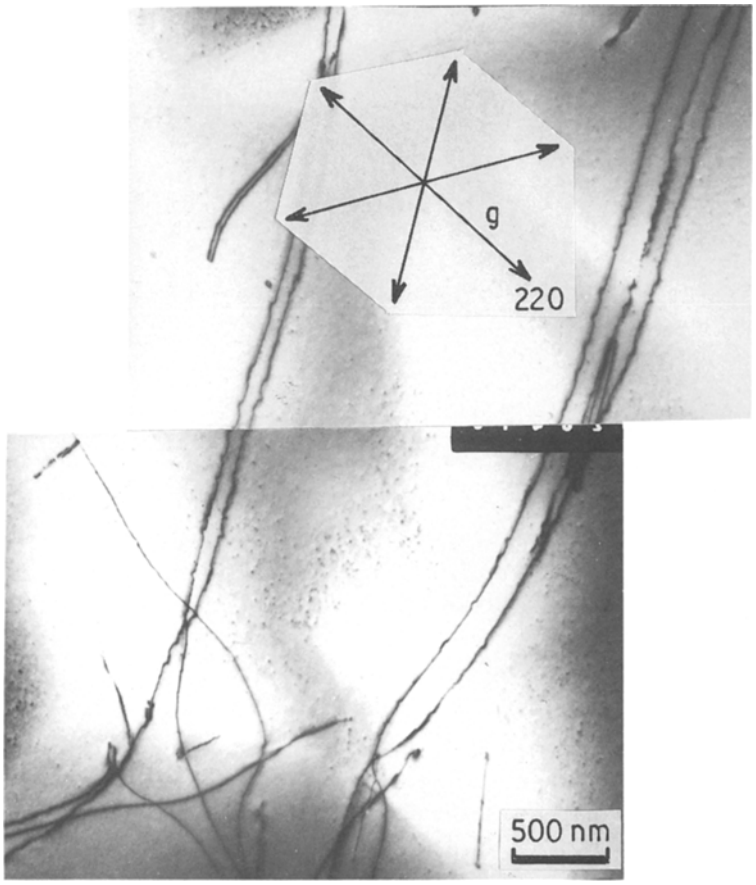

Figure 8 Example of a typical dislocation arrangement in a $Cd_{0.66}Hg_{0.34}Te$ sample deformed at 449 K.

energy ⟨110⟩ valleys of the glide plane. Individual screws or 60° dislocation segments are also observed, see Fig. 7b.

At higher temperatures, the dislocation density is homogeneous. Figure 8 is a representative feature of the structure at 449 K ($\tau \approx 4.7$ MPa, $\gamma \approx 4\%$). Dislocations are large and lie in dipole configuration near the ⟨110⟩ directions. Edge dipoles parallel to ⟨112⟩ are also observed.

(ii) $x = 0.2$

At room temperature ($\tau \approx 8$ MPa, $\gamma \approx 4\%$) the dislocation structure observed at 200 KV contains long segments of near screw orientation and 60° dislocations. Frequently they are not rigorously straight and tend to form edge dipoles, as can be seen in Fig. 9a. This configuration type, which has also been observed by Orlova *et al.* [25] on deformed CdTe at room temperature ($T \approx 0.217\,T_M$), can be due to jogs dragging on the screws. Under the action of the electron beam irradiation, dislocation motion has also been noticed and could explain the waved aspect of dislocations as well as their varied orientations observed in some cases. Observations at 100 KV confirm the screw or 60° character of straight dislocations, Fig. 9b. Numerous defects also present in this last one are probably introduced by ion milling.

When the deformation temperature increases dislocations are less and less aligned along ⟨110⟩ directions and the dipole density strongly increases.

(iii) Stacking fault energy

Weak-beam images of 60° dislocations in $x = 0.2$ and 0.66 samples are shown in Figs 10a and b respectively. Dislocations are dissociated into two Shockley partials 1/6⟨112⟩. The dissociation width does not depend on the x composition and was found to be between 9 and 11 nm. The stacking fault energy γ calculated using anisotropic elasticity [26] has been found to be:

$$\gamma = 12 \pm 2\,\mathrm{mJ\,m^{-2}}$$

This value is in a good agreement with those of II–VI binary compounds. The reduced stacking fault energy

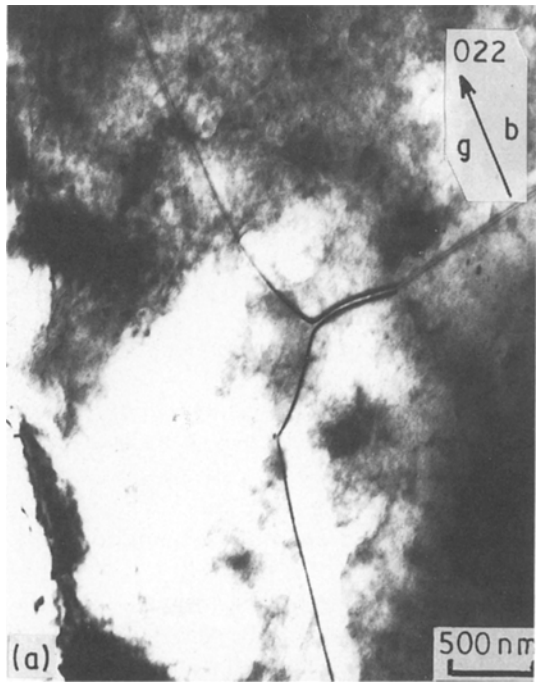

Figure 9 $Cd_{0.2}Hg_{0.8}Te$ deformed at room temperature. (a) Observation at 200 KV, and (b) observation at 100 KV.

Figure 9 Continued.

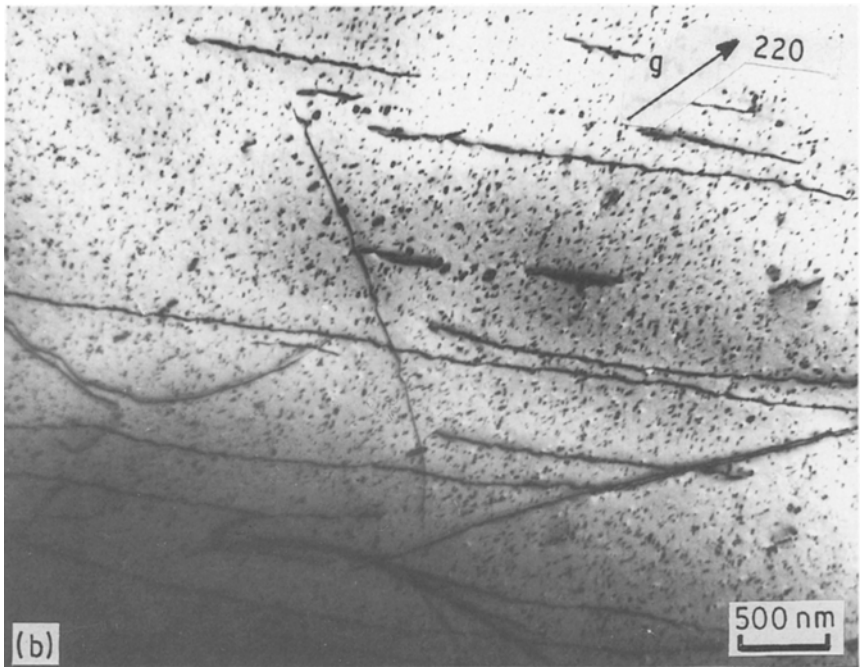

γ' according to the definition of Gottschalk [27] ($\gamma' = \gamma \cdot q$ with $q = (\sqrt{3}/4)a^2$) is $\gamma' = 12.5 \pm 1$ meV atom^{-1}.

6. Conclusion

Vickers hardness measurements are made over all composition range ($0 \leqslant x \leqslant 1$) as function of temperature ($300 \leqslant T \leqslant 630$ K). Experimental H_v values show, for about $x \approx 0.7$, a maximum whose amplitude decreases as the temperature increases. The empirical relations proposed describe quite well the $H_v(x, T)$ experimental hardness variations. The hardness peak is typical of a pseudo-binary solid solution system. However, the hypothesis of an ordering on the sublattice, as firstly suggested by Balagurova *et al.* [14] can not be ruled out.

From our uniaxial stress measurements we are able to give a first contribution to the knowledge of deformation mechanisms acting in the CMT alloys, and to the characterization of dislocation substructures induced during deformation. Our experimental results show that the deformation is thermally activated. At "low" temperatures activation volumes are small ($V < 100\ b^3$), potential barriers ΔG_0 are high and dislocations are oriented along $\langle 1\,1\,0 \rangle$ directions. These different points are characteristic of a Peierls mechanism. At "higher" temperatures, the mechanism is less well defined, dislocations then gathered into dipoles and multipoles and the activation volumes are high. In addition dislocations are dissociated with a stacking fault energy $\gamma \approx 12 \pm 2$ mJ m^{-2}. This value is in good agreement with those previously found in other II–VI binary compounds for which γ seems to be independent of the material ionicity. Moreover, though the mechanical properties of CMT (H_v, τ^*_{Ly} and ΔG_0) are composition dependent, the dissociation width remains constant.

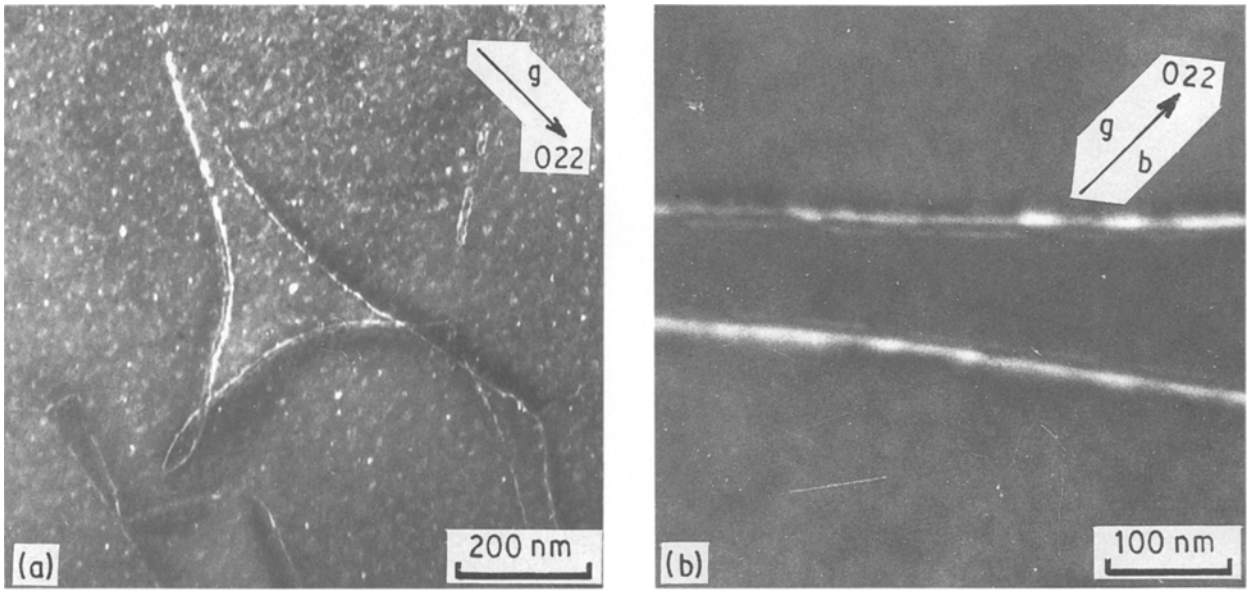

Figure 10 Dissociated dislocations (a) $Cd_{0.2}Hg_{0.8}Te$ and (b) $Cd_{0.66}Hg_{0.34}Te$.

References

1. E. Y. GUTMANAS, N. TRAVITZKY and P. HAASEN, *Phys. Stat. Solidi* (*a*) **51** (1979) 435.
2. E. Y. GUTMANAS and P. HAASEN, *Phys. Stat. Solidi* (*a*) **63** (1981) 193.
3. G. RIVAUD and J. C. DESOYER, *J. Phys. Paris* **44** (1983) 387.
4. G. RIVAUD, M. F. DENANOT, H. GAREM and J. C. DESOYER, *Phys. Stat. Solidi* (*a*) **73** (1982) 401.
5. YU. A. OSIP'YAN and V. F. PETRENKO, *Soviet. Phys. JETP* **48** (1978) 147.
6. C. LEVADE, J. J. COUDERC, I. DUDOUIT and J. GARIGUE, *Phil. Mag.* **A54** (1986) 259.
7. J. C. PHILLIPS, "Bond and Bands in Semiconductors" (Academic Press, New York, 1973) p. 43.
8. J. F. BARBOT, G. RIVAUD and J. C. DESOYER, *J. Mater. Sci.* **23** (1988) 1655.
9. S. COLE, M. BROWN and A. F. W. WILLOUGHBY, *J. Mater. Sci.* **20** (1985) 274.
10. J. F. BARBOT, G. RIVAUD, C. BLANCHARD, J. C. DESOYER and D. LE-SCOUL, to be published in "Materials in Electronics".
11. J. F. BARBOT, Thesis, Poitiers University (1988).
12. M. SCHENK and A. FISSEL, *J. Cryst. Growth* **86** (1988) 502.
13. S. COLE, M. BROWN and A. F. W. WILLOUGHBY, *J. Mater. Sci.* **17** (1982) 2061.
14. E. A. BALAGUROVA and E. KHABARO, *J. Sov. Phys.* **7** (1976) 943.
15. D. B. ZAX, S. VEGA, N. YELLIN and D. ZAMIR, *Chem. Phys. Lettr.* **138** (1987) 105.
16. P. GROH, "Dislocations et déformation plastique", (Yravals 1979) France (Les éditions de Physique 1980).
17. J. J. GILMAN, *J. Appl. Phys.* **46** (1975) 5110.
18. O. OMRI, Thesis, Nancy University (1981).
19. M. KARMOUDA, Thesis, Lille University (1984).
20. P. GALL, J. P. PEYRADE, R. COQUILLE, F. REYNAUD, S. GABILLET and A. ALBACETE, *Acta Metall.* **35** (1987) 143.
21. P. BOIVIN, Thesis, Poitiers University (1988).
22. D. QUELARD, Thesis, Toulouse Univeristy (1987).
23. G. RIVAUD, private communication.
24. K. MAEDA, K. NAKAGAWA and S. TAKEUCHI, *Phys. Status. Solidi* (*a*) **48** (1978) 370.
25. R. ORLOVA and B. SIEBER, *Acta Metall.* **32** (1984) 1045.
26. J. P. HIRSCH and J. LOTHE, "Theory of dislocations" McGraw Hill, 2nd Edition (Wiley, New York, 1982).
27. H. GOTTSCHALK, G. PARKER and H. ALEXANDER, *Phys. Status Solidi* (*a*) **45** (1978) 207.

Received 12 December 1988
and accepted 17 July 1989